A safe and effective modification of Thomson's jumping ring experiment

2012 Eur. J. Phys. 33 1625

(http://iopscience.iop.org/0143-0807/33/6/1625)

IOP Publishing European Journal of Physics
Eur. J. Phys. **33** (2012) 1625–1634 doi:10.1088/0143-0807/33/6/1625

A safe and effective modification of Thomson's jumping ring experiment

Felix Waschke, Andreas Strunz and Jan-Peter Meyn

Department für Physik, Friedrich-Alexander-Universität Erlangen-Nürnberg, Didaktik der Physik, Staudtstraße 7, D-91058 Erlangen, Germany

E-mail: jan-peter.meyn@physik.uni-erlangen.de

Received 20 June 2012, in final form 6 August 2012
Published 12 September 2012
Online at stacks.iop.org/EJP/33/1625

Abstract
The electrical circuit of the jumping ring experiment based on discharging a capacitor is optimized. The setup is scoop proof at 46 V and yet the ring jumps more than 9 m high. The setup is suitable for both lectures and student laboratory work in higher education.

(Some figures may appear in colour only in the online journal)

1. Introduction

The jumping ring experiment by Elihu Thomson (1853–1937) is an instructive demonstration. It has given rise to an impressive number of didactic publications [1–11].

The original demonstration in 1887 was to show that an ac current is capable of mechanical work. Didactic versions of the experiment, however, are primarily used to illustrate Lenz's law. Aside from the theoretical issues discussed in the cited work, a convincing jumping height seems to be a continuous challenge. Under the guise of showing the influence of lower ring conductivity, the ring is often cooled in liquid nitrogen in order make a pleasant experiment amazing. Obviously, it would be fairer to show two independent phenomena such as induction and low resistance at cryogenic temperature in separate experiments.

Although we are not aware of any fatal accident in a lecture hall, we are convinced that many existing setups are justifiably called dangerous due to the use of line voltage or charged high voltage capacitors in a self-made apparatus. Under the constraint of scoop-proof voltage of less than 46 V according to regulations [12], we have optimized an apparatus by taking into account both theoretical and practical aspects, for any of the components. The jumping height of 9 m exceeds the ceiling height of a typical lecture hall. The apparatus serves any introductory physics course at university level, while its construction is a suitable students' project. In the following section, we briefly summarize the physics behind the ring experiment, as necessary for the optimization procedure described in section 3.

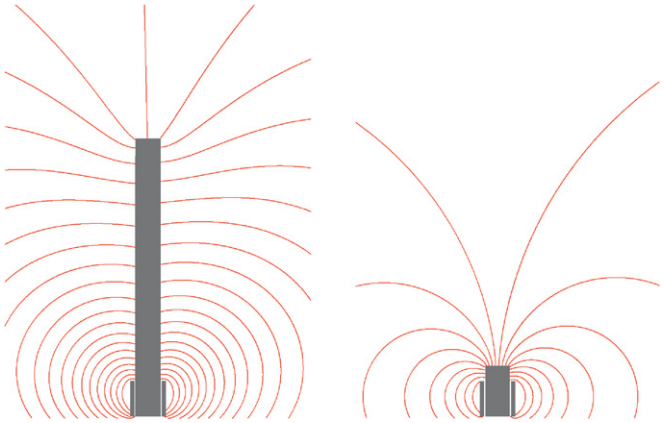

Figure 1. Magnetic field lines (red) around the iron core with coil (grey), calculated with *Feldlab* [13]. The radial field section is stretched by a longer iron rod.

2. Physics of the jumping ring experiment

An iron rod is transiently magnetized by a coil with an ac power supply. An aluminium ring is lying loosely on the coil. Due to the increase of magnetic flux by turning on the current in the coil, a current is induced inside the ring. The magnetic moment of the ring current is opposite to the magnetic moment of the coil and the ring is repelled. This is called a demonstration of Lenz's law.

However, after a quarter ac period, the current has reached its maximum and starts to decrease. The magnetic field decreases and the current in the ring is reversed while the sign of the rod's magnetic moment remains. Therefore, the ring is attracted. From the jumping height, one can estimate the maximum velocity of the ring, and the time it takes to leave the magnetized rod. In practical cases, it requires much more than a quarter ac cycle at 50 Hz for the ring to leave. Hence, the simple Lenz' law explanation is insufficient. A net force averaged over several cycles—which is clearly present in any ac jumping ring experiment—is only possible because of the phase shift of the magnetic flux and the ring current, caused by the ring's inductance [1, 9].

The simplified explanation is open to criticism for another reason: a dipole is not accelerated in a homogeneous external field. Therefore, a long iron rod should be less efficient to repel the ring than a coil filled with a short iron core, because the latter geometry has a more inhomogeneous field. In fact, only the radial component of the iron rod's magnetic field causes acceleration: together with the ring current it causes a Lorentz force in the direction of the ring axis [2]. The advantage of a long iron rod is the extension of the radial field component along the path of acceleration, as shown in figure 1.

3. Setup and optimization

3.1. Scaling

The size of the experiment is determined by the diameter of the iron core, 30 mm. This dimension is similar to most experiments described in the literature. The apparatus is large enough for a lecture hall and yet small enough for easy handling and storage in a cabinet.

3.2. Current source

According to regulations [12], the maximum ac voltage for a scoop-proof laboratory apparatus is 46 V amplitude, or 33 V effective. This value is a factor of 7 below the line voltage of 230 V. In order to create a sufficient magnetic field, the current must not be smaller than in the 230 V case. A lower voltage at a constant current implies a lower resistance of the coil and hence a careful layout. Moreover, if the usual jumping height of below 1 m is considered insufficient for a striking demonstration, the current must be much larger than the typical 10 to 20 A. Since the current is only required for milliseconds, a power supply for continuous operation such as a welding transformer is a very inefficient solution.

A large electrolyte capacitor can deliver a pulsed current of the order of 10 kA. Although small and affordable, the current rating of the capacitor is superior to any reasonable continuous mode ac power supply. The capacitor with capacity C and the coil with inductance L form a resonant circuit, delivering an alternating current when switched together. Since the electrolyte capacitor must not be charged against its polarity, the resonant circuit has to be switched off after the first half oscillation. The energy of the capacitor, charged at voltage U, is transferred to the coil according to

$$\tfrac{1}{2}CU^2 = \tfrac{1}{2}LI^2. \tag{1}$$

The current amplitude is therefore

$$I = U\sqrt{\frac{C}{L}}. \tag{2}$$

In order to achieve a high current, the capacitance C must be as large as is reasonable. We use a single electrolyte capacitor rated 0.45 F at 63 V maximum voltage, the largest model in stock of the manufacturer[1]. The use of a capacitor charged with a dc power supply enables us to stretch the limit for the safety regulation, which is 70 V for a dc source. It is very unlikely that anybody would touch open contacts during the milliseconds of operation. For the characterization, we use 63 V as allowed by the capacitor specification and leave it to the user to decide about the ac or dc nature of the electrical hazard.

3.3. Coil

3.3.1. Steady-state current analysis. The coil's magnetic field should be as large as possible. The field amplitude H is given by the current I, the number of coil windings N and the length l_c,

$$H = \frac{NI}{l_c}. \tag{3}$$

At given voltage U, the current is limited by the ohmic resistance of the coil wire. For the magnetic field, it is irrelevant whether the current in the individual parts of the coil flows in a parallel or a serial circuit. A coil is constructed of N rings of cross section A_c and length l_{cturn}, see figure 2. In series, the resistance is $R_{\mathrm{ser}} = N\rho_{Cu}A_c l_{\mathrm{cturn}}$, while in parallel the resistance is $R_{\mathrm{par}} = (1/N)\rho_{Cu}A_c l_{\mathrm{cturn}}$. The current ratio is

$$\frac{I_{\mathrm{par}}}{I_{\mathrm{ser}}} = \frac{\frac{U}{R_{\mathrm{par}}}}{\frac{U}{R_{\mathrm{ser}}}} = \frac{R_{\mathrm{ser}}}{R_{\mathrm{par}}} = N^2. \tag{4}$$

For the parallel circuit of coil turns, $N = 1$ and hence

$$\frac{H_{\mathrm{par}}}{H_{\mathrm{ser}}} = \frac{1}{N}\frac{I_{\mathrm{par}}}{I_{\mathrm{ser}}} = N. \tag{5}$$

[1] FTCAP GmbH, Nedderweg 10, 25813 Husum, Germany. www.ftcap.de.

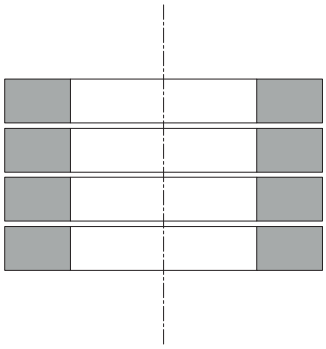

Figure 2. For a given amount of copper and coil size, $N = 4$ turns may be in series or combined in parallel to a single turn.

The magnetic field at a given voltage is larger for a coil of few windings of thick wire. This result is counter-intuitive since electromagnet fields are usually associated with coils of many turns. In practice one cannot go for a single-turn coil because of the finite internal resistance of the current source; the latter must be smaller than the coil resistance. This consideration is exact for a long coil, and in principle also valid for a short coil of given geometry, i.e. length and thickness of the copper package.

Winding a coil of a few turns of thick wire leaves more air than is theoretically necessary. For example, a round wire yields in practice a tighter package than a rectangular wire, despite the theoretical advantage of the latter. Finally, the parasitic resistance of line feeds, switch and capacitor becomes relevant for very low coil resistance, but their values can only roughly be estimated to be of the order mΩ. The fine tuning of the coil must therefore rely on trial and error. Enamelled copper wire with 4 mm diameter is a workable compromise between stiffness and conductivity. The most effective coil in our experiment is 30 mm (one core diameter) high and has $N = 13$ turns in two layers with an ohmic resistance of $R = 2.4$ mΩ.

3.3.2 Transient current analysis. For the resonant circuit, the inductance L and the coil's impedance have to be taken into account. In analogy to the comparison of parallel and serial coil turns in the previous section, one finds that the damping factor $R_c/2L$ is constant for a fixed geometry, i.e. the number of turns or the inductance does not matter. However, with a given capacitor, the resonance frequency ω_0 is larger at lower inductance L. This is a benefit, because the current I and the derivative of the B-field are larger, and so is the acceleration. The total momentum of the ring is transferred over a shorter distance closer to the coil, where the B-field and its time derivative are largest. The conclusion to use as few coil turns as possible is in agreement with the consideration on dc resistance in the previous section.

3.3.3. Mechanical stability. The large rate magnetic field variation compresses the coil and reduces the momentum transfer to the ring. We have fixed the coil with a plexiglass plate bolted to the table. This measure seems to be insignificant at first sight, but it improves the jumping height by more than 30%—that is, for example, 8 m instead of 6 m. The final coil was brushed with epoxy glue to further enhance its stability.

The plate also serves as a right base for the ring, so that its axis is aligned with the iron rod. If the ring hung only loosely on the coil, its acceleration would not be parallel to the iron core and it would lose momentum due to friction.

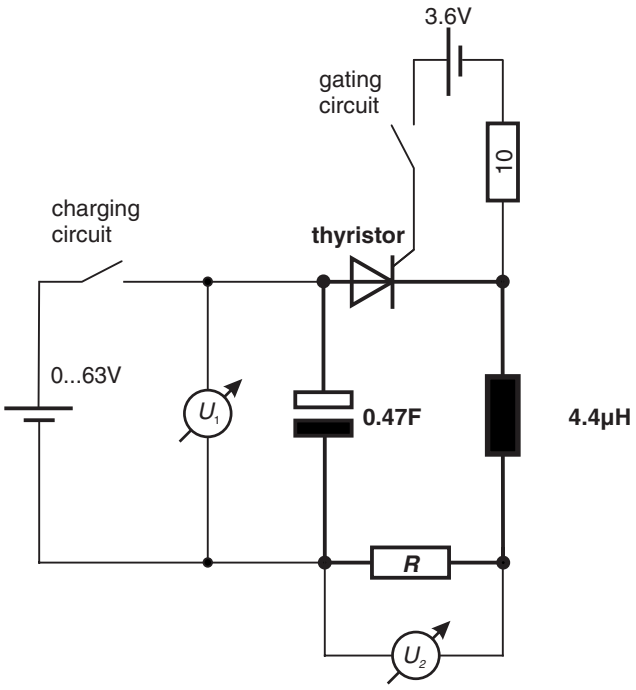

Figure 3. Complete circuit of the experiment with the resonant circuit highlighted. The capacitor is charged when the power supply is switched on and the thyristor is gated by switching on the 3.6 V battery. For characterization, the voltages U_1 and U_2 can be monitored.

3.4. Switch

A peak current of the order of 10 kA is a heavy load for regular mechanical switches. A semiconductor switch has no moving part, no interfaces to air and therefore a lower internal resistance. We used the high-power thyristor Semikron SKET 330.[2] The thyristor has the additional advantage of inhibiting reverse poling harmful to the electrolyte capacitor by acting as a diode. This switching off happens smoothly when the current approaches zero, so no spike of the induced voltage occurs. The thyristor is gated by 3.6 V, 360 mA from a battery which is switched mechanically. The circuit diagram is shown in figure 3.

Electrical connection of the resonant circuit is realized by an enamelled copper sheet sized 16 mm × 2 mm. The filed ends are connected with standard iron screws. Flexible copper cables with crimped cable shoes are also usable but yield a 10% lower jumping height due to higher contact resistance.

3.5. Circuit characterization

The circuit layout is based on the goal of achieving a very large current ramp by minimizing the ohmic resistance. Characterization is carried out without the iron core so that the nonlinear magnetization has not been taken into account.

[2] Thyristor SKET 330/12, manufactured by SEMIKRON Elektronik GmbH & Co. KG, Sigmundstrasse 200, 90431 Nürnberg, Germany. www.semikron.de.

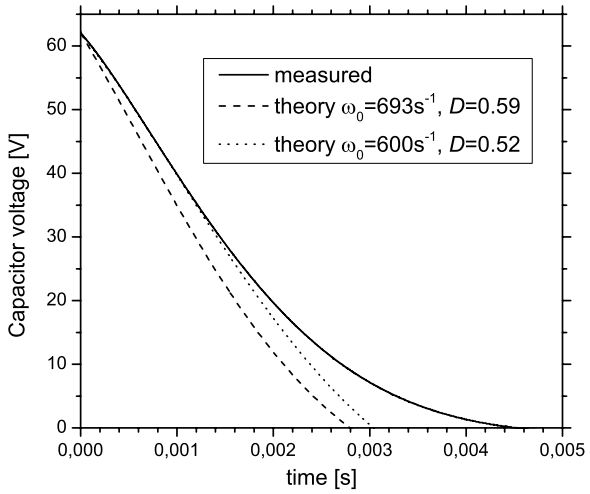

Figure 4. Capacitor voltage compared to the solution of the differential equation for the electrical charge.

The capacitance of the capacitor was measured as $C = 0.47$ F from the time constant of discharging over a 10Ω resistor. The inductance of the coil was measured as 4.4 μH by combining it with a 1 μF foil capacitor, excitation with an air coupled external coil driven by a function generator and reading the frequency of maximum amplitude. With these values, the current amplitude of the undamped *LC*-circuit would be 20 kA according to equation (2).

The voltage between different points of the circuit, as shown in figure 3, is monitored as a function of time with an educational data acquisition system, CASSY2.[3] The current is measured as the voltage across a 118 mm long piece of the line feed between the capacitor and coil. The measurement line is fit into a sawn slit and fixed by cold forging. The line resistance of 0.065 mΩ is determined from the voltage with a 10 A test current. It coincides well with the value 0.063 mΩ calculated from dimensions. In the same manner, the total ohmic resistance without the switch is measured as 2.67 mΩ. The expected value from the copper dimension is 2.60 mΩ, of which the coil contributes 2.37 mΩ. The contact resistance at the connectors' interfaces is therefore almost negligible. The resistance of the switch is nonlinear, and there is a constant voltage drop at the pn-junction. At high current, the internal differential resistance of the switch is 0.18 mΩ.

The ohmic resistance of the complete coil circuit including the capacitor's internal resistance is estimated by discharging the capacitor over a twisted wire instead of a coil, so that the inductance is negligible. The nonlinear decay curve indicates a nonlinear internal resistance of the capacitor. An exponential fit to the higher voltage part of the curve yields a total resistance 3.6 mΩ. Since the copper wire and switch contribute 2.85 mΩ, the internal capacitor's resistance is of the order 0.75 mΩ. The measured values for C and L yield $\omega_0 = 693\ \mathrm{s}^{-1}$ without the damping term. The damping constant, $R/2L = 407\ \mathrm{s}^{-1}$, is smaller than ω_0 by a factor $D = 0.59$, i.e. the damping is below critical.

The voltage and current as a function of time are shown in figures 4 and 5. Compared to the theoretical curves, the temporal shape is faster and the maximum current of 8.6 kA is smaller than the theoretical value of 13 kA. A better overlap between theory and measurement

[3] LD Didactic GmbH, Leyboldstr. 1, 50354 Hürth, Germany. www.ld-didactic.de.

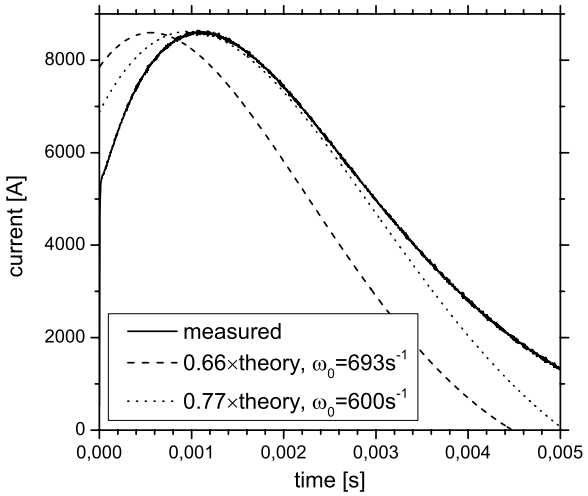

Figure 5. Current compared to the solution of the differential equation.

is obtained with lower $\omega_0 = 600\ \mathrm{s}^{-1}$ and $D = 0.52$. The latter values would imply a modified value for $L = 5.9\ \mu\mathrm{H}$ and the same total ohmic resistance of 3.6 mΩ. The error caused by the nonlinear behaviour of the switch and capacitor is of the order of 20%, i.e. the model of the simple linear resonant circuit is acceptable for much of the first half oscillation. Only when the voltage approaches zero does the thyristor become very nonlinear and inhibit the expected overshooting.

The peak power $P = UI$ of 400 kW punctuates the statement that the electrolyte capacitor is a quite powerful electrical source on a short timescale.

3.6. Iron rod

Many setups for the ring experiment use an iron core made from insulated iron wires in order to avoid eddy current. A circular iron core is usually made from a bundle of wires with the disadvantage of reduced maximum magnetization due to voids. Transformer cores made from an insulated sheet usually come in quadratic cross section, which is an impractical shape. A solid iron core made from standard mild steel S355J2+N is the simplest effective solution. It is fixed with an M6 headless screw to the baseplate.

The B-field of the empty coil was measured with a CASSY sensor as 16 mT in the centre with a dc current of 44 A. Extrapolating to the peak current of 7.8 kA in the iron-filled coil yields a maximum H-field of the order of $2.2 \times 10^6\ \mathrm{A\ m}^{-1}$, respective $B = 2.8$ T. At the jumping ring's initial position, $H = 0.95 \times 10^6\ \mathrm{A\ m}^{-1}$ and $B = 1.2$ T. Even at this lower field strength, the iron core is almost saturated. It is therefore not possible to provide a simple dynamical model for the iron core. The magnetic field B in the iron rod is measured by time integrating the voltage signal of a sensor coil with ten turns and twisted signal wires, under the assumption of homogenous flux in the cross section. The sensitivity of the coil was calibrated against a commercial B-field sensor (see footnote 3). Figure 6 shows the result for different heights above the coil. The flux is much larger in the lower part of the core. This measurement supports the statement in section 3.3.2 that a high oscillation frequency of the LC-circuit is beneficial, because in a faster acceleration phase the ring propagates less far away from the region of highest B-field.

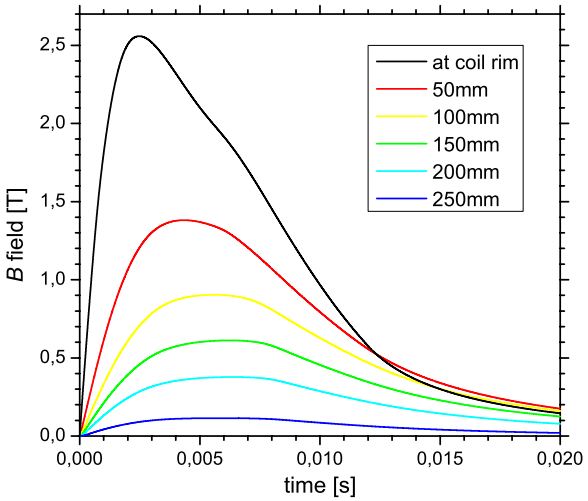

Figure 6. Longitudinal component of the *B*-field at various heights above the coil. The *B*-field was calculated by time integrating the induced voltage of a sensor coil tightly wound over the iron core at the specified height under the assumption of uniform magnetic flux within the cross section. The field is stronger in the lower part of the core, making a high oscillation frequency of the coil circuit more effective. Note the retardation at larger height, indicating a strong magnetic after-effect.

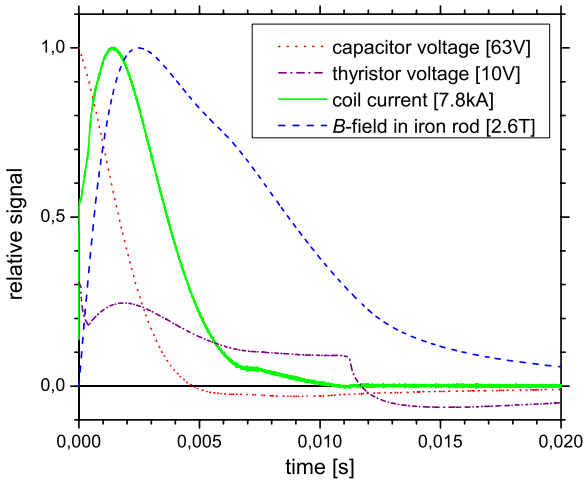

Figure 7. Scaled capacitor voltage, thyristor voltage, coil current and *B*-field in the iron core at the initial ring position.

Figure 7 shows the magnetic flux together with the voltage and current. Both figures 6 and 7 indicate that the magnetization is a complex process in time and space. We left the detailed analysis of this phenomenon as a subject for future research and we optimized the length of the iron core empirically. Best results were obtained with a 300 mm long core, which protrudes 250 mm above the coil rim. This is much longer than expected: during the short time interval of positive $\dot{B}(t)$ the ring ascends only a few centimetres, so it is exposed to negative $\dot{B}(t)$ and consequently negative force while moving over the upper part of the iron

Table 1. Accumulation of improvements over the initial version of the experiment after general layout. Although the starting values are rather arbitrary, the idea of taking care of several minor issues to gain a huge factor in performance is obvious.

Coil parameters N, A_c	1.5
Coil fixture	1.3
Replacing mechanical switch by thyristor	1.9
Copper sheet cable	1.1
Iron core annealing	1.2
Ring annealing	1.5
Ring dimension	1.5
Total	11

core. However, the radial field component decreases by a factor of 5 within the first 50 mm. By the time the force changes sign, the ring has ascended into a region of weaker radial B-field and the influence of Lorentz force is small.

The magnetic properties of the iron core are improved by annealing at 450 °C so that the jumping height is increased by 20% . Even higher temperature has no significant advantage.

3.7. Ring

The optimum ring dimension has been studied in detail for continuous ac propulsion [5, 11]. In the present case, the iron core is saturated and aerodynamics are significant due to the large initial speed. Empirically, the ring dimensions turned out not to be very critical, and the best rings vary with jumping height. The highest jumps were obtained with 35 mm inner diameter, 5 mm wall thickness and 15 mm height. The mass of an aluminium ring of that size is 27 g. The ring rests on a levelled launch pad with a groove centred to the axis of the rod. Due to the unavoidable asymmetry of the magnetic field, the ring still may touch the rod, but the trajectory is much more stable than for a ring launched hanging loosely on the first coil turn. Actually, the groove is machined into the plate used for compressing the coil as described in section 3.3.3. Aluminium for general machining purpose contains a few per cent of copper to improve mechanical strength. The electrical conductivity of alloy EN-AW 2007 is $\sigma = 2.2 \times 10^7\ \Omega\mathrm{m}^{-1}$ compared to $\sigma = 3.7 \times 10^7\ \Omega\mathrm{m}^{-1}$ for pure aluminium. Increasing the jumping height by annealing has been described in [10] and [11]. Several rings turned from EN-AW 2007 rods have been annealed for 6 h and cooled slowly in the oven. Best results in terms of jumping height were found at 350 °C and 400 °C, and only minor deterioration at 450 °C.

4. Conclusion

The jumping ring experiment is constructed under the constraint of the scoop-proof voltage. A photograph of the setup is shown in figure 8. By using fewer and thicker turns for the primary coil, the current is increased and the magnetization is as strong as for a coil with many thin turns at a hazardous voltage level. An electrolyte capacitor delivers a peak current of more than 8 kA. The resonant circuit comprised of the capacitor and the coil is switched by a thyristor. Oscillation stops after the first-half period because the thyristor acts as a diode. A number of technical improvements, each gaining a moderate increase in jumping height, yield a convincing result. In table 1 we provide some factors of improvement over the first version of the experiment to illustrate the effectiveness of combining a larger number of relatively small improvements. At 46 V, which is a scoop-proof voltage for both ac and dc regulations,

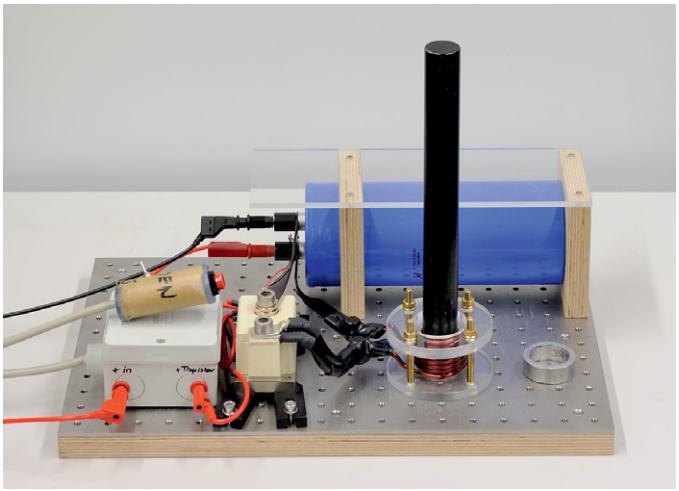

Figure 8. Setup of the jumping ring experiment on a small nonmagnetic baseplate 30 cm ×45 cm. The ring is removed to make visible the circular groove in the plexiglass launch pad above the coil. The blue capacitor is protected against damage from falling rings by a plexiglass cover. The grey box on the left contains a battery for gating the thyristor by pressing the button lying on top. For charging the capacitor, any short circuit protected source can be used (not shown).

the jumping height exceeds 9 m. At the technical limit of 63 V, still considered safe under dc regulations, the ring repeatedly jumps higher than 12 m.

Acknowledgments

We thank Ferdinand Bund at Isodraht GmbH for kindly sending us a substantial amount of copper in form of various wires, in several boxes, always as a gift. The staff of the workshop of Physikalisches Institut machined and annealed several batches of rings and cores and took it in their stride that only a few parts went into the final setup though all were workmanlike. Gesine Murphy took care of the language.

References

[1] Churchill E J and Noble J D 1971 A demonstration of Lenz' law? *Am. J. Phys.* **39** 285–7
[2] Sumner D J and Thakkrar A K 1972 Experiments with a 'jumping ring' apparatus (undergraduate exercise) *Phys. Educ.* **7** 238
[3] Saslow W M 1987 Electromechanical implications of Faraday's law: a problem collection *Am. J. Phys.* **55** 986–93
[4] Ford P J and Sullivan R A L 1991 The jumping ring experiment revisited *Phys. Educ.* **26** 380
[5] Schneider C S and Ertel J P 1998 A classroom jumping ring *Am. J. Phys.* **66** 686–92
[6] Tjossem P J H and Cornejo V 2000 Measurements and mechanisms of Thomson's jumping ring *Am. J. Phys.* **68** 238–44
[7] Tanner P, Loebach J, Cook J and Hallen H D 2001 A pulsed jumping ring apparatus for demonstration of Lenz's law *Am. J. Phys.* **69** 911–6
[8] Bostock-Smith J M 2008 The jumping ring and Lenz's law—an analysis *Phys. Educ.* **43** 265
[9] Jeffery R N and Amiri F 2008 The phase shift in the jumping ring *Phys. Teach.* **46** 350–7
[10] Baylie M, Ford P J, Mathlin G P and Palmer C 2009 The jumping ring experiment *Phys. Educ.* **44** 27
[11] Tjossem P J H and Brost E C 2011 Optimizing Thomson's jumping ring *Am. J. Phys.* **79** 353–8
[12] Deutsche Norm: Sicherheitsbestimmungen für elektrische Mess-, Steuer-, Regel- und Laborgeräte Teil 1: Allgemeine Anforderungen *IEC 61010-1:2001* (German version of *EU Regulation* EN 61010-1:2001)
[13] Suleder M 2003 *Elektrische und Magnetische Felder* (Stuttgart: Klett) (A CD-ROM with the software Feldlab is part of the booklet)